БІОФІЗИКА КЛІТИНИ

УДК 577.37

FLUORESCENCE ENERGY TRANSFER STUDY OF THE LIPID BILAYER INTERACTIONS WITH TRUNCATED APOLIPOPROTEIN A-I MUTANTS

M.S. Girych[1], I.L. Maliyov[1], M.V. Romanova[1], G.P. Gorbenko[1], E. Adachi[2], C. Mizuguchi[2], J. Molotkovsky[3], H. Saito[2]

[1]*V. N. Karazin Kharkiv National University, 4 Svobody Sq., 61022, Kharkiv, Ukraine*
[2]*Institute of Health Biosciences and Graduate School of Pharmaceutical Sciences, The University of Tokushima, 1-78-1 Shomachi, Tokushima 770-8505, Japan*
[3]*Institute of Bioorganic Chemistry, Russian Academy of Sciences, 16/10 Miklukho-Maklaya, Moscow, 117871, Russia*
email:girichms@gmail.com
Submitted May 7, 2013
Accepted June 2, 2013

Förster resonance energy transfer (FRET) between anthrylvinyl-labeled phosphatidylcholine (AV-PC) as a donor and Thioflavin T (ThT) as an acceptor has been employed to explore the binding of N-terminal fragments of wild (A83) and amyloidogenic variants of apolipoprotein A-I (apoA-I) with substitution mutations G26R, G26R/W@8, G26R/W@50 and G26R/W@72 to the model membranes composed of phosphatidylcholine (PC). Analysis of the experimental data in terms of 2D FRET model combined with the partition model revealed that ThT distance from the lipid bilayer center falls in the range 1.7-2.5 nm, suggesting that the dye is located in the interfacial membrane region, at the level of phospholipid headgroups, while partition coefficient characterizing ThT distribution between the aqueous and lipid phases was estimated to be *ca*. 4×10^2. Interaction of monomeric apoA-I N-terminal fragments with PC liposomes resulted in the increase of AV-ThT FRET efficiency, while this parameter displayed ambiguous behavior upon membrane binding of fibrillar apoA-I mutants. These findings were rationalized in terms of the existence of discrete lipid-binding sites within the fibril structure. It was demonstrated that FRET technique can be employed for ascertaining specific modes of fibril-membrane interactions.
KEY WORDS: Förster resonance energy transfer, lipid bilayer, Thioflavin T, apolipoprotein A-I.

ВЗАЄМОДІЯ МУТАНТІВ АПОЛІПОПРОТЕЇНУ А-І З ЛІПІДНИМ БІШАРОМ ЗА ДАНИМИ ІНДУКТИВНО-РЕЗОНАНСНОГО ПЕРЕНОСУ ЕНЕРГІЇ

М.С. Гірич[1], І.Л. Малійов[1], М.В. Романова[1], Г.П. Горбенко[1], Е. Адачі[2], С. Мізугучі[2], Ю.Г. Молотковський[3], Х. Сайто[2]

[1]*Харківський національний університет імені В.Н. Каразіна, майдан Свободи, 4, Харків, 61022*
[2]*Інститут Здоров'я та Факультет фармацевтичних наук Університету Токушими, Токушима 770-8505, Японія*
[3]*Інститут біоорганічної хімії Російської академії наук, вул. Міклухо-Маклая, 16/10, 117871, Росія*
Ферстеровський перенос енергії (ФПЕ) між антрілвінілміченим фосфатидилхоліном (AV-PC) у якості донора та Тіофлавіном Т (ThT) у якості акцептора був застосований для дослідження зв'язування N-термінального фрагменту дикого типу (A83) та амілоїдогенних варіантів аполіпопротеїну А-І (apoA-I) з мутаційними заміщеннями G26R, G26R/W@8, G26R/W@50 та G26R/W@72, з модельними мембранами із фосфатидилхоліну (PC). Аналіз експериментальних даних в рамках 2D моделі ФРЕТ комбінованої з моделлю розподілу, показав, що ThT локалізується на поверхні розділу ліпід-вода, на відстані 1.7-2.5 нм від центру ліпідного бішару, а коефіцієнт розподілу цього барвника між водною та ліпідною фазами становить *ca*. 4×10^2. Взаємодія мономерного N-термінального фрагменту apoA-I з PC ліпосомами призводила до зростання ефективності ФПЕ, тоді як при зв'язуванні фібрилярних мутантів apoA-I з мембранами поведінка цього параметру була неоднозначною. Висловлено припущення про існування дискретних ліпід-зв'язуючих центрів у структурі фібрил. Продемонстровано, що метод ФПЕ може бути застосований для визначення специфічних механізмів взаємодії амілоїдних фібрил з мембранами.
КЛЮЧОВІ СЛОВА: Ферстеровський перенос енергії, ліпідний бішар, Тіофлавін Т, аполіпопротеїн А-І.

ВЗАИМОДЕЙСТВИЕ МУТАНТОВ АПОЛИПОПРОТЕИНА A-I С ЛИПИДНЫМ БИСЛОЕМ ПО ДАННЫМ ИНДУКТИВНО-РЕЗОНАНСНОГО ПЕРЕНОСА ЭНЕРГИИ

М.С. Гирич[1], І.Л. Малиёв[1], М.В. Романова[1], Г.П. Горбенко[1], Е. Адачи[2], С. Мизугучи[2], Ю.Г. Молотковский[3], Х. Сайто[2]

[1]Харьковский национальный университет имени В.Н. Каразина, пл. Свободы, 4, Харьков, 61022
[2]Институт Здоровья и Факультет фармацевтических наук Университета Токушимы, Токушима 770-8505, Япония
[3]Институт биоорганической химии Российской академии наук, ул. Миклухо-Маклая, 16/10, 117871, Россия

Фёрстеровский перенос энергии (ФПЭ) между антрилвинилмеченым фосфатидилхолином (AV-PC) в качестве донора и Тиофлавином Т (ThT) в качестве акцептора был применен для исследования связывания N-терминального фрагмента дикого типа (A83) и амилоидогенных вариантов аполипопротеина A-I (apoA-I) с мутационными замещениями G26R, G26R/W@8, G26R/W@50 и G26R/W@72, с модельными мембранами из фосфатидилхолина (PC). Анализ экспериментальных данных в рамках 2D модели ФПЭ, комбинированной с моделью распределения, показал, что ThT локализуется на поверхности раздела липид-вода, на расстоянии 1.7-2.5 нм от центра липидного бислоя, а коэффициент распределения этого красителя между водной и липидной фазами составляет *ca*. 4×10^2. Взаимодействие мономерного N-терминального фрагмента apoA-I с PC липосомами приводило к возрастанию эффективности ФПЭ, тогда как при связывании фибриллярных мутантов apoA-I с мембранами поведение этого параметра было неоднозначным. Высказано предположение о существовании дискретных липид-связывающих центров в структуре фибрилл. Продемонстрировано, что метод ФПЭ может быть использован для выяснения специфических механизмов взаимодействия амилоидных фибрилл с мембранами.

КЛЮЧЕВЫЕ СЛОВА: Фёрстеровский перенос энергии, липидный бислой, Тиофлавин Т, аполипопротеин A-I.

The past decades have seen drastic upsurge in the interest to abnormal protein aggregation into highly ordered beta-sheet fibrillar structures (amyloids), involved in molecular etiology of a number of so-called protein misfolding disorders, *viz.* Alzheimer's, Parkinson's, Huntington's diseases, type II diabetes, rheumatoid arthritis, spongiform encephalophaties, systemic amyloidoses, etc. [1-3]. Toxic action of this kind of protein aggregates is thought to be largely determined by the impairment of cell membranes [4-6]. Despite great advances in the understanding of fibril-membrane interactions, little is known about the driving forces and molecular-scale details of this process. In the present study we focused our efforts on characterization of membrane-associating properties of different mutant forms of apolipoprotein A-I (apoA-I) N-terminal fragment in both monomeric and fibrillar states. Addressing this problem is of great importance in view of the association of apoA-I with various hereditary systemic amyloidoses and atherosclerosis where protein-lipid interactions underlie the molecular etiology of such disorders [7-9].

To gain insight into membrane-associating properties of fibrillar apoA-I, we employed the model systems, containing phosphatidylcholine (PC) liposomes doped with 0.3 mol% fluorescent lipid 1-acyl-2-[12-(9-anthryl)-11*E*-dodecenoyl]-*sn*-glycero-3-phosphocholine (AV-PC) and N-terminal fragments of wild (A83) and amyloidogenic apoA-I variants with substitution mutations G26R, G26R/W@8, G26R/W@50 and G26R/W@72 in pre-fibrillar and fibrillar states.

MATERIALS AND METHODS

The N-terminal 1-83 fragment of human apoA-I G26R and its single tryptophan variants G26R/W@8, G26R/W@50 and G26R/W@72 were expressed and purified as described earlier [10]. Since two extra amino acids, Gly and Ser, are attached at the amino terminus of the target apoA-I, the two residues preceding the normal apoA-I sequence are numbered −1 and −2. The apoA-I preparations were at least 95% pure as assessed by SDS-PAGE.

In all experiments, apoA-I variants were freshly dialyzed from 6M guanidine hydrochloride solution into 10 mM Tris buffer (150 mM NaCl, 0.01 % NaN3, pH 7.4) before use. The reaction of apoA-I fibrillization was conducted at 37 °C in the above buffer with constant agitation on an orbital shaker. The amyloid nature of fibrillar aggregates was confirmed in Thioflavin T (ThT) assay [11].

Large unilamellar vesicles were prepared from PC using extrusion technique. A thin lipid film was obtained by removing the organic solvent (chloroform) under a stream of nitrogen. The dry lipid residues were subsequently hydrated with the above buffer at room temperature to yield lipid concentration of 1 mM. Thereafter, the sample was subjected to 15 passes through a 100-nm pore size polycarbonate filter (Millipore, Bedford, USA). AV-PC (0.3 mol % of total lipid) was added to PC prior to the solvent evaporation. The concentration of fluorescent lipid was determined spectrophotometrically using anthrylvinyl extinction coefficient 9×10^3 $M^{-1}cm^{-1}$ at 367 nm [12].

Fluorescence measurements were performed with a LS-55 spectrofluorimeter equipped with a magnetically stirred cuvette holder (Perkin-Elmer Ltd., Beaconsfield, UK) using 10 mm path-length quartz cuvettes. The AV fluorescence was excited at 367 nm. Förster resonance energy transfer (FRET) experiments were conducted after pre-incubation of PC-liposomes with N-terminal fragment variants of apoA-I. The efficiency of energy transfer (E) was determined by measuring the decrease of AV fluorescence upon addition of ThT: $E = 1 - Q_{DA} / Q_D = 1 - Q_r$, where Q_D and Q_{DA} are the donor quantum yields in the absence and presence, respectively, of acceptor, and Q_r is the relative quantum yield.

The critical distance of energy transfer (in nm) was calculated as [13]:

$$R_0 = 2.11\cdot10^{-2}\left(\kappa^2 n_r^{-4} Q_D J\right)^{1/6},\ J = \int_0^\infty F_D(\lambda)\varepsilon_A(\lambda)\lambda^4 d\lambda \Big/ \int_0^\infty F_D(\lambda) d\lambda \qquad (1)$$

where J is the overlap integral derived from numerical integration (in $M^{-1}cm^{-1}nm^4$), $F_D(\lambda)$ is the donor fluorescence intensity, $\varepsilon_A(\lambda)$ is the acceptor molar absorbance at the wavelength λ, n_r is the refractive index of the medium (n_r=1.4), Q_D is the donor quantum yield, κ^2 is an orientation factor. Assuming random reorientation of the donor emission and acceptor absorption transition moments during the emission lifetime (κ^2 = 0.67), R_0 value was estimated to be 3.4 nm for AV – ThT donor-acceptor pair (with Q_D= 0.15 for AV). Fluorescence intensity measured in the presence of ThT at the maximum of AV emission (430 nm) was corrected for reabsorption and inner filter effects using the following coefficient [14]:

$$k = \frac{(1-10^{-A_o^{ex}})(A_o^{ex}+A_a^{ex})}{(1-10^{-(A_o^{ex}+A_a^{ex})})A_o^{ex}} \frac{(1-10^{-A_o^{em}})(A_o^{em}+A_a^{em})(A_o^{em}+A_a^{em})}{(1-10^{-(A_o^{em}+A_a^{em})})A_o^{em}} \qquad (2)$$

where A_o^{ex}, A_o^{em} are the donor optical densities at the excitation and emission wavelengths in the absence of acceptor, A_a^{ex}, A_a^{em} are the acceptor optical densities at the excitation and emission wavelengths, respectively.

RESULTS AND DISCUSSION

Analysis of FRET between AV and ThT in lipid systems

As illustrated in Fig. 1, AV fluorescence progressively decreases with increasing ThT concentration, suggesting that excitation energy is transferred from the donor (AV) to the

acceptor (ThT). The occurrence of FRET is also corroborated by the fact that relative quantum yield of the donor decreases at lower lipid concentrations (Fig. 2). This implies that acceptor surface density becomes higher with decreasing the volume of lipid phase accessible to ThT, thereby resulting in the enhancement of energy transfer. Strong overlap between AV emission and ThT absorption spectra yields the Förster radius ca. 3.4 nm, as calculated from Eq. (1).

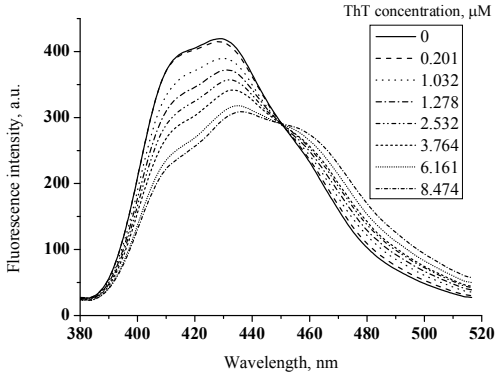

Fig. 1. Fluorescence spectra illustrating FRET between AV-PC and ThT.

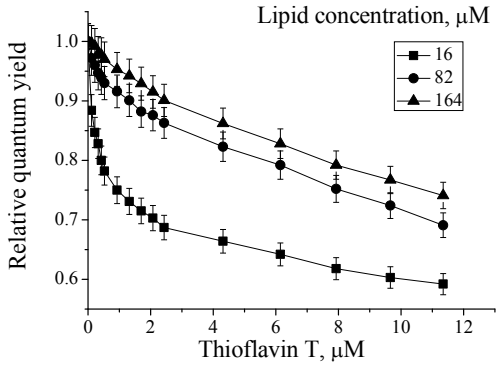

Fig. 2. The efficiency of energy transfer between AV-PC and ThT measured at varying lipid concentrations.

The results of FRET measurements have been quantitatively interpreted in terms of the model of energy transfer on a surface proposed by Fung & Stryer [15] and extended in our previous studies [16] to allow for distance dependence of orientation factor in two-dimensional systems. Assuming that donors and acceptors are randomly distributed in different planes separated by a distance d_a, the efficiency of energy transfer is given by:

$$E = 1 - \int_0^\infty \exp(-\lambda)\exp\left(-C_a^s S(\lambda)\right) d\lambda \tag{3}$$

$$S(\lambda) = \int_{d_a}^\infty \left[1 - \exp\left(-\lambda\left(\frac{R_o}{R}\right)^6\right)\right] 2\pi R dR \tag{4}$$

where $\lambda = t/\tau_D$, τ_D is the lifetime of excited donor in the absence of acceptor, R_o is the Förster radius, C_a^s is the concentration of acceptors per unit area related to the molar concentrations of the fluorescent lipids (L_{AV}) and total lipids (L_o):

$$C_a^s = \frac{L_{AV}}{L_o S_{PC}} \tag{5}$$

Here S_{PC} is the mean area per PC molecule taken as 0.65 nm^2.

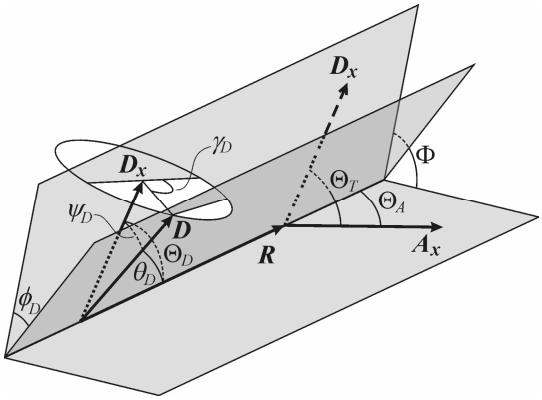

Fig. 3. Angular relationships between the donor emission and acceptor absorption transition moments.

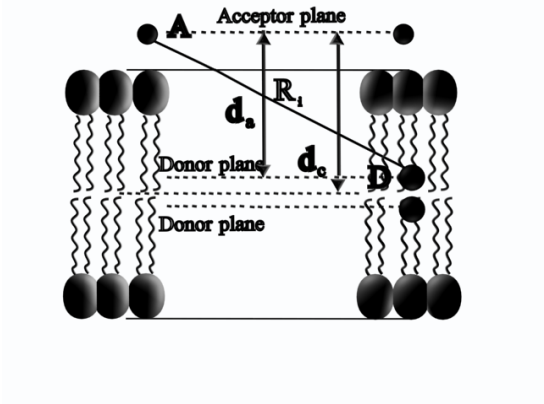

Fig. 4. Schematic representation of planar arrangement of donors and acceptors in a lipid bilayer.

Orientation factor κ^2 can be represented as:

$$\kappa^2 = (\sin\theta_D \sin\theta_A \cos\phi - 2\cos\theta_D \cos\theta_A)^2 \tag{6}$$

where θ_D and θ_A are the angles between the donor emission (**D**) or acceptor absorption (**A**) transition moments and the vector **R** joining the donor and acceptor (Fig. 3), ϕ is the dihedral angle between the planes (**D, R**) and (**A, R**). The applicability of Eq. (6) is limited to the case where the vectors **D** and **A** do not undergo any reorientation during the transfer time. Alternatively, Förster radius should be calculated using the dynamic average value of orientation factor ($\langle\kappa^2\rangle$) [17]. If the donor emission and acceptor absorption transition moments are symmetrically distributed within the cones about certain axes $\mathbf{D_x}$ and $\mathbf{A_x}$, $\langle\kappa^2\rangle$ is given by:

$$\langle\kappa^2\rangle = (\sin\Theta_D \sin\Theta_A \cos\Phi - 2\cos\Theta_D \cos\Theta_A)^2 \langle d_D^x\rangle\langle d_A^x\rangle + 1/3(1-\langle d_D^x\rangle) + 1/3(1-\langle d_A^x\rangle) + \\ + \cos^2\Theta_D \langle d_D^x\rangle(1-\langle d_A^x\rangle) + \cos^2\Theta_A \langle d_A^x\rangle(1-\langle d_D^x\rangle) \tag{7}$$

where Θ_D and Θ_A are the angles made by the axes $\mathbf{D_x}$ and $\mathbf{A_x}$ with the vector **R**, Φ is the angle between the planes containing the cone axes and the vector **R**, $\langle d_D^x\rangle$ and $\langle d_A^x\rangle$ are so-called axial depolarization factors:

$$\langle d_{D,A}^x\rangle = 3/2\langle\cos^2\psi_{D,A}\rangle - 1/2 \tag{8}$$

where $\psi_{D,A}$ are the cone half-angles. These factors are related to the steady-state (r) and fundamental (r_0) anisotropies of donor and acceptor:

$$d_{D,A}^x = \pm(r_{D,A}/r_{0D,A})^{1/2} \tag{9}$$

When the donor and acceptor planar arrays are located at different levels across the membrane, multiple donor-acceptor pairs are involved in energy transfer, so that orientation factor appears to be a function of the donor-acceptor separation (**R**). Particularly, for the most probable membrane orientation of $\mathbf{D_x}$ and $\mathbf{A_x}$, parallel to the bilayer normal, the angles Θ_D and Θ_A made by $\mathbf{D_x}$ and $\mathbf{A_x}$ with **R** are equal and depend on the distance between donor and acceptor ($\Theta_A = \Theta_D = \theta$, $\theta = f(R)$). Under these circumstances Eq.(7) can be rewritten in the form:

$$\left\langle \kappa^2(\theta) \right\rangle = \left\langle d_D^x \right\rangle \left\langle d_A^x \right\rangle (3\cos^2\theta - 1)^2 + 1/3(1 - \left\langle d_D^x \right\rangle) + \\ + 1/3(1 - \left\langle d_A^x \right\rangle) + \cos^2\theta(\left\langle d_D^x \right\rangle - 2\left\langle d_D^x \right\rangle \left\langle d_A^x \right\rangle + \left\langle d_A^x \right\rangle) \quad (10)$$

where $\cos^2\theta = (d_a / R)^2$. Next, by representing Förster radius as $R_o = [\kappa^2(R)]^{1/6} \cdot R_o^r$ one obtains:

$$S(t) = \int_{d_a}^{\infty} \left[1 - \exp\left(-\lambda \kappa^2(R) \left(\frac{R_o^r}{R} \right)^6 \right) \right] 2\pi R dR; \quad R_o^r = 2.11 \cdot 10^{-2} \left(n_r^{-4} Q_D J \right)^{1/6} \quad (11)$$

In analyzing the FRET data presented here we considered the lipid and lipid-protein systems as containing two donor planes separated by a distance d_t and one acceptor plane located at a distance d_c from the membrane center (Fig. 4). Given that for the outer acceptor plane $d_a = |d_c - 0.5d_t|$ while for the inner plane $d_a = d_c + 0.5d_t$, the following relationships hold:

$$S_1(\lambda) = \int_{|d_c - 0.5d_t|}^{\infty} \left[1 - \exp\left(-\lambda \kappa_1^2(R) \left(\frac{R_o^r}{R} \right)^6 \right) \right] 2\pi R dR \quad (12)$$

$$S_2(\lambda) = \int_{d_c + 0.5d_t}^{\infty} \left[1 - \exp\left(-\lambda \kappa_2^2(R) \left(\frac{R_o^r}{R} \right)^6 \right) \right] 2\pi R dR \quad (13)$$

$$\kappa_{1,2}^2(R) = \left\langle d_D^x \right\rangle \left\langle d_A^x \right\rangle \left(3\left(\frac{d_c \mp 0.5d_t}{R} \right)^2 - 1 \right) + \frac{1 - \left\langle d_D^x \right\rangle}{3} + \frac{1 - \left\langle d_A^x \right\rangle}{3} + \\ + \left(\frac{d_c \mp 0.5d_t}{R} \right)^2 (\left\langle d_D^x \right\rangle - 2\left\langle d_D^x \right\rangle \left\langle d_A^x \right\rangle + \left\langle d_A^x \right\rangle) \quad (14)$$

$$E = 1 - 0.5 \times \left(\int_0^{\infty} \exp(-\lambda) \exp\left[-C_a^s S_1(\lambda) \right] d\lambda + \int_0^{\infty} \exp(-\lambda) \exp\left[-C_a^s S_2(\lambda) \right] d\lambda \right) \quad (15)$$

where S_1 and S_2 are the quenching contributions describing energy transfer from the outer and inner donor planes, respectively. The relationships (12)-(15) are valid when the donor and acceptor transition moments are distributed about the axes $\mathbf{D_x}$ and $\mathbf{A_x}$ parallel to the bilayer normal **N**. If this is not the case, additional depolarization factors accounting for the deviations of $\mathbf{D_x}$ and $\mathbf{A_x}$ from **N** should be introduced: $d_{D,A}^a = \frac{3}{2}\cos^2\alpha_{D,A} - \frac{1}{2}$, where $\alpha_{D,A}$ are the angles made by $\mathbf{D_x}$ and $\mathbf{A_x}$ with **N**. By applying the Soleillet's theorem stating the multiplicativity of depolarization factors, Eq. (14) may be rewritten in a more general form:

$$\kappa_{1,2}^2(R) = d_D d_A \left(3\left(\frac{d_c \mp 0.5d_t}{R} \right)^2 - 1 \right) + \frac{1 - d_D}{3} + \frac{1 - d_A}{3} + \\ + \left(\frac{d_c \mp 0.5d_t}{R} \right)^2 (d_D - 2d_D d_A + d_A) \quad (16)$$

where $d_{D,A} = \left\langle d_{D,A}^x \right\rangle d_{D,A}^a$.

Acyl bearing AV fluorophore, 12-(9-anthryl)-11-*trans*-dodecenoyl, which do not possess any polar group in its chain; tends to fully immerse into hydrophobic core of a lipid bilayer. ^{1}H-NMR measurements showed that AV-PC induces upfield shift of the proton resonances at

the level of terminal CH_3 groups and C4-C13 methylenes, exerting no effect on the resonances of choline protons [18]. This observation indicates that AV fluorophore is localized at the level of terminal methyl groups, preferentially orienting parallel to acyl chains. To allow for the dependence of energy transfer efficiency on the surface acceptor concentration (Eqs. (3)-(5)), ThT binding to PC bilayer was quantified in terms of partition model, with the dye partition coefficient (K_p) defined as:

$$K_p = \frac{N_L^{'} V_W}{N_W^{'} V_L} \tag{17}$$

where $N_L^{'}$, $N_W^{'}$ are the moles of the dye in the lipid and aqueous phases, respectively; V_L, V_W are the volumes of these phases. The volume of lipid phase was calculated as:

$$V_L = N_A C_L \sum \nu_i f_i \tag{18}$$

here C_L is the molar lipid concentration, f_i is mole fraction of the i-th bilayer constituent, ν_i is its molecular volume taken as 1.58 nm^3 for PC. Under the employed experimental conditions ($C_L <$ 1mM) the V_L value is much less than total volume of the system ($V_t = 1\,dm^3$), so that $V_W \approx V_t$.

Combination of the above FRET and partition models allowed us to extract both structural (d_c) and binding (K_p) parameters from the least-squares fitting of the experimental data. These parameters were optimized with the separation between the outer and inner AV planes (d_t) taken as 0.3 nm (Fig. 4). Since orientation of lipid-bound ThT molecule is unknown, the FRET data were analyzed under two limiting assumptions α_A=0 and α_A=π/2, corresponding to parallel and perpendicular disposition of the absorption transition moment with respect to lipid bilayer surface. Presented in Fig. 5 is the best-fitting curve calculated for the largest of the employed lipid concentrations. Ultimately, the data fitting procedure yielded the following sets of optimizing parameters: α_A=0, K_p = (4.3±0.7)×10^2, d_c=1.7±0.2 and α_A=π/2, K_p = (4.1±0.6) ×10^2, d_c = 2.5±0.3. These estimates, suggesting that ThT is located in the interfacial bilayer region at the level of PC headgroups, seem to be quite reasonable, since positively charged moiety of the dye may hamper its insertion into hydrophobic membrane core.

Analysis of FRET between AV and ThT in lipid-protein systems

At the next step of the study we addressed the question of whether membrane binding of monomeric and fibrillar apoA-I variants may manifest itself in the changes of AV-ThT FRET. Since the highest ThT density is attained in the headgroup bilayer region, it might be expected that membrane association of monomeric proteins or much more bulky structures like oligomers and amyloid fibrils would dramatically affect the efficiency of energy transfer, especially if such structures have an ability to specifically interact with the acceptor (ThT). Indeed, our FRET studies revealed some differences in membrane interactions of apoA-I variants (Fig. 6).

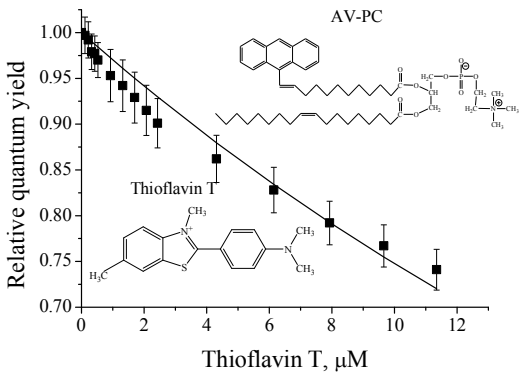

Fig. 5. FRET profile measured at lipid concentration 164 μM. Solid line represents theoretical curve calculated in terms of the combined FRET-partition model for $\alpha_A = \pi/2$, $K_p = (4.1 \pm 0.6) \times 10^2$, $d_c = 2.5 \pm 0.3$

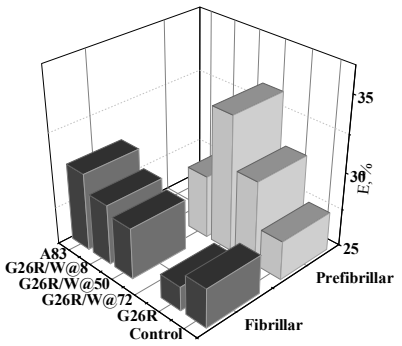

Fig. 6. The efficiency of energy transfer between AV-PC and ThT in protein-lipid systems

As follows from electron paramagnetic resonance studies [19], monomeric wild-type 1-83 apoA-I N-terminal fragment in a membrane-bound state possesses two amphipathic alpha-helices (6-34 and 50-83) which seem to attach to lipid bilayer via their hydrophobic surfaces and intermediate unstructured (35-39) and beta-sheet (40-49) sites. The Iowa mutation G26R gives rise to destabilization of 6-34 alpha-helix and, as a consequence, the 1-50 fragment of monomeric 1-83 G26R has a random coil structure, but nevertheless 1-83 apoA-I keeps the ability of attaching to lipid bilayer in the similar way as the wild-type because the 50-83 alpha-helix remains undisturbed [20,21]. Moreover, as seen in Fig. 7, the upper surface of 50-83 alpha-helix, oriented toward the aqueous phase, contains the cluster of negatively charged amino acid residues that may be the ThT binding site with rather high affinity, as has been recently demonstrated [22]. Next, based on the above estimates of ThT binding characteristics, it was of interest to assess what changes in the acceptor surface density may account for the observed protein-induced alterations in FRET efficiency. As schematically depicted in Fig. 8, assuming parallel orientation of ThT (with dimension *ca*. 1.6 nm), relative to 50-83 alpha-helix (with the length 3.2 nm), such binding site can adopt only one or two ThT molecules and our model considers both possibilities. Since alpha-helix has the diameter about 1.2 nm and its hydrophobic part is embedded into lipid bilayer, the actual distance between AV and ThT bound to such alpha-helix would be less than 3 nm, i.e. less than Forster radius (3.4 nm), suggesting the possibility of FRET increase in the case of association of 1-83 apoA-I with liposomes doped with AV-PC.

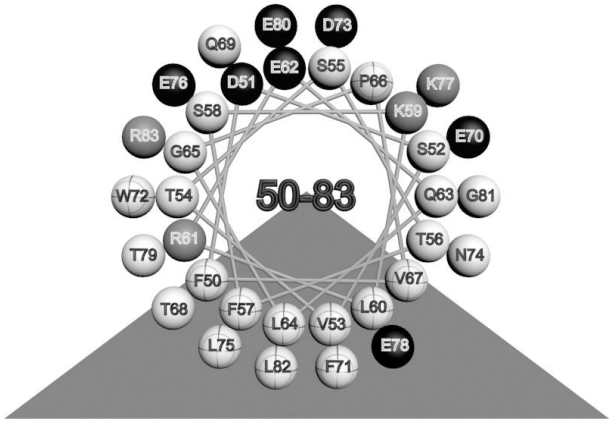

Fig. 7. Edmundson helical wheel analysis of the 50–83 α-helical region within the apoA-I sequence. Helical projections were generated assuming a perfect-helical periodicity of 3.6 residues per helical turn. The color code is crossed-white for hydrophobic, white for polar and uncharged, black for negatively charged, and grey for positively charged residues. Prediction of the orientation of the amphipathic wheels was solely based on clustering of the hydrophobic residue on a sector of the wheel. The apolar and polar solvation space is represented by grey and white backgrounds, respectively.

Indeed, as illustrated in Fig. 6, pre-incubation of PC liposomes with monomeric apoA-I variants resulted in the increase of FRET efficiency. Table 1 represents the estimates of the acceptor surface density (C_a^s) and fraction of bound protein (f_{bound}) obtained for PC (control) and PC-protein systems on the assumption that monomeric fragment can adopt either 1 or 2 ThT molecules. The monomeric G26R/W@72 variant brings about the highest increase in FRET efficiency and, accordingly, has the highest affinity for lipid bilayer where around 6% of the total protein is associated with liposomal membranes. For the examined monomeric apoA-I variants P_{bound} value decreases in the order G26R/W@72 > G26R > G26R/W@50.

Table 1.

Acceptor surface density (C_a^s) and fraction of bound protein (f_{bound}) estimated for monomeric and fibrillar (*) apoA-I variants associating with PC liposomes

System	C_a^s (1.7), nm^{-2}	C_a^s (2.5), nm^{-2}	f_{bound}/1ThT (1.7), %	f_{bound}/1ThT (2.5), %	f_{bound}/2ThT (1.7), %	f_{bound}/2ThT (2.5), %
Control (PC)	0.0132	0.0121	0	0	0	0
G26R	0.0152	0.0138	2.74	2.50	1.37	1.25
G26R/W@50	0.0147	0.0131	2.14	1.52	1.07	0.76
G26R/W@72	0.0173	0.0158	5.79	5.29	2.90	2.65
A83*	0.0153	0.0140	3.04	2.77	1.52	1.39
G26R*	0.0126	0.0115	0	0	0	0
G26R/W@8*	0.0141	0.0129	1.29	1.18	0.65	0.59
G26R/W@50*	0.0142	0.0129	1.33	1.21	0.66	0.61

These discrepancies can be explained by the different fibrillogenic propensity of the apoA-I mutants, presented in Fig.9 in terms of the fibril formation kinetics. Fibrillization was the slowest for G26R/W@72 suggesting that the predominant part of incubated proteins do not aggregate into prefibrillar nuclei whereas the part of monomeric G26R and G26R/W@72 can be excluded from lipid binding by this process. Interestingly, G26R/W@50 and G26R display close fibrillogenic propensities but FRET is significantly lower in the case of G26R/W@50. This may result from the disturbance of 50-83 alpha-helix by the substitution of Trp72 with Phe, followed by the decrease in ThT affinity for the binding sites on this structure.

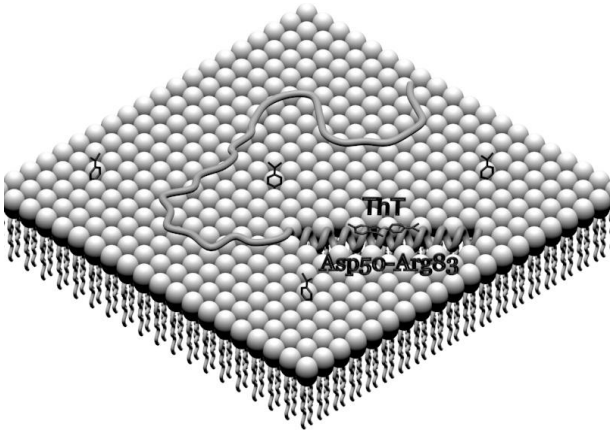

Fig. 8. Tentative mode of the interaction between monomeric 1-83 apoA-I variant and PC bilayer

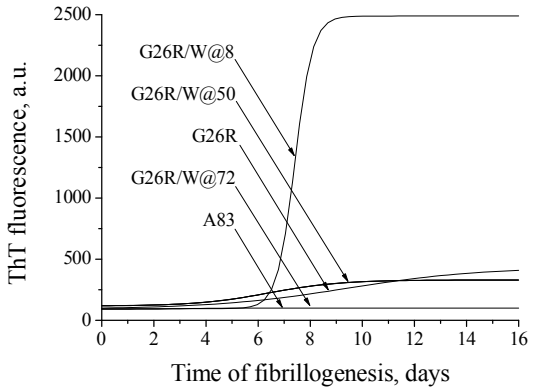

Fig. 9. Fibrillization kinetics of of apoA-I variants monitored by measuring the increase in ThT fluorescence

As shown in Fig. 6, FRET efficiencies in the protein-lipid systems containing fibrillar apoA-I variants display somewhat ambiguous but very interesting behavior. Given that the depth of AV bilayer location is *ca*. 2 nm, while the diameter of apoA/G26R fibrils is *ca*. 10 nm, it follows that in the areas of fibril-liposome contact the distance between the AV moiety and the external surface of fibrils can be as large as 12 nm, the distance, at which energy transfer becomes negligible.

It is worth noting, that, according to our estimates, the apoA-I fibrils have only one principal ThT binding site located in the groove formed by Thr16 and Tyr18 (Fig. 10), with binding stoichiometry ($n = 0.18$), corresponding to one dye molecule per about 5 protein monomers. However, even if the groove-containing surface is oriented towards the lipid surface there would be no possibility for these grooves to be occupied by ThT, because the proteins were incubated with liposomes prior to the dye addition. Really, incubation of PC liposomes with fibrillar G26R resulted in the FRET decrease (about 4.5%). Allowing for the width of G26R fibrils, it follows that the liposome external surface area nearly 300 nm^2 is excluded from ThT-liposome interaction. This area corresponds to ~ 30 nm of fibril length for one PC liposome. There are two additional arguments in favor of the possibility of such interactions. On the one hand, amyloid fibril bending rigidity is nearly 2.41×10^{-25} Nm^2 which precisely allows the wrapping of it around 100 nm liposome [23]. On the other hand, if one assumes that almost all G26R/W@8 molecules are in a fibrillar state, the content of G26R/W@50 fibrils must be 5-fold lower, with ~ 43 nm of fibrillar length per one liposome, as schematically depicted in Fig. 11. On the contrary, in the case of G26R/W@8 and G26R/W@50 we observed increase of acceptor surface density which may arise from different morphology of apoA-I amyloid fibrils [24]. Given that amyloid fibril structure is characterized by the coiling mode of protofibrils, some of ThT molecules located in the grooves of G26R/W@8 and G26R/W@50 fibrils may appear within the radius of FRET, producing the increase in energy transfer efficiency. As for A83, it does not readily form true amyloid fibrils, because there was no increase in ThT fluorescence. Therefore, A83 sample can contain monomeric, oligomeric and aggregated species that presumably enhance FRET in the same manner as monomeric apoA-I variants.

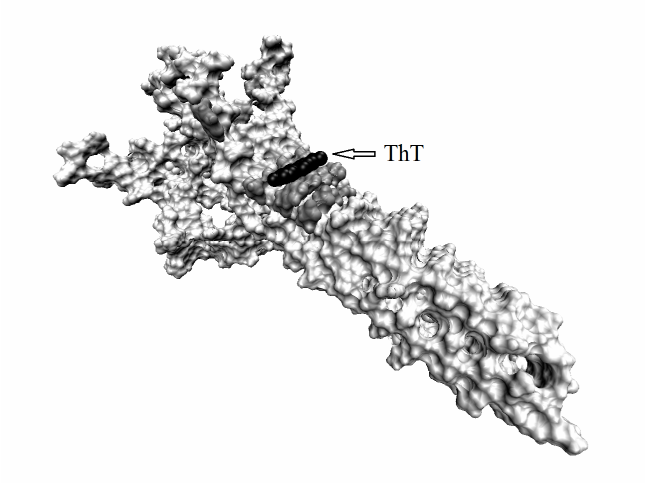

Fig. 10. 3D structure of tetrameric G26R/W@8 apoA-I variant in a fibrillar state derived from Rosetta calculations. Shown in black is ThT molecule.

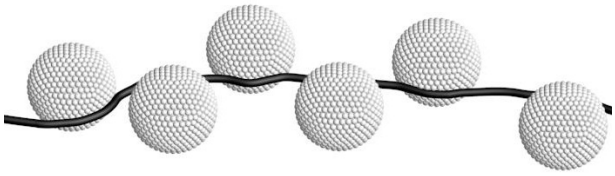

Fig. 11. Illustration of multiple adsorption of liposomes on amyloid fibril.

CONCLUSIONS

In summary, principal findings of the present study can be outlined as follows.

(1) Analysis of FRET between AV-PC (donor) and ThT (acceptor) in terms of 2D FRET model combined with partition model revealed that ThT distance from the lipid bilayer center falls in the range 1.7-2.5 nm, suggesting that the dye is located in the interfacial membrane region, at the level of phospholipid headgroups, while partition coefficient characterizing ThT distribution between the aqueous and lipid phases was estimated to be *ca*. 4×10^2.

(2) Interaction of monomeric apoA-I N-terminal fragments with PC liposomes resulted in the increase of AV-ThT FRET efficiency being in inverse relation to fibrillogenic propensity.

(3) FRET efficiencies in the protein-lipid systems containing fibrillar apoA-I variants display ambiguous behavior, suggesting the possibility of different amyloid fibril morphology and the existence of discrete lipid-binding sites within the fibril structure.

Overall, the present study demonstrates that FRET technique can be effectively employed for clarifying the precise modes of fibril-membrane binding. Although translation of the above findings into the membrane effects of apoA-I amyloid fibrils in vivo is not immediate, they may prove of significance in creating a solid background for understanding membrane-related mechanisms that underlie the molecular etiology of various hereditary systemic amyloidoses and atherosclerosis associated with apoA-I.

ACKNOWLEDGEMENTS

The work was supported by the grant from the Fundamental Research State Fund (project number F54.4/015).

REFERENCES

1. Chiti F. Protein misfolding, functional amyloid, and human disease / F. Chiti, C. M. Dobson // Annu. Rev. Biochem. – 2006. – V. 75. – P. 333–366.
2. Stefani M. Generic cell dysfunction in neurodegenerative disorders: role of surfaces in early protein misfolding, aggregation, and aggregate cytotoxicity / M. Stefani // Neuroscientist. – 2007. – V. 13(5). – P. 519–531.

3. Greenwald J. Biology of Amyloid: Structure, Function, and Regulation / J. Greenwald, R. Riek // Structure. – 2010. – V. 18. – P. 1244–1260.
4. Kinnunen P. K. J. Amyloid formation on lipid membrane surfaces / P. K. J. Kinnunen // Open Biol. J. – 2009. – V. 2. – P. 163–175.
5. The two-fold aspect of the interplay of amyloidogenic proteins with lipid membranes / A. Relini, O. Cavalleri, R. Rolandi, A. Gliozzi // Chem. Phys. Lipids. – 2009. – V. 158(1). – P. 1–9.
6. Stefani M. Biochemical and biophysical features of both oligomer/fibril and cell membrane in amyloid cytotoxicity / M. Stefani // FEBS J. – 2010. – V. 277(22). – P. 4602–4613.
7. Komoda T. The HDL Handbook. Biological Functions and Clinical Implications / T. Komoda. - Academic Press, 2010.
8. Ramirez-Alvarado M. Protein Misfolding Diseases: Current and Emerging Principles and Therapies / M. Ramirez-Alvarado, J. W. Kelly, C. M. Dobson. – John Wiley & Sons, Inc., 2010.
9. Sarantseva S. Amyloidosis - Mechanisms and Prospects for Therapy / S. Sarantseva // Intech., 2011.
10. Dual role of an N-terminal amyloidogenic mutation in apolipoprotein A-I: destabilization of helix bundle and enhancement of fibril formation / E. Adachi, H. Nakajima, C. Mizuguchi [et al.] // J. Biol. Chem. – 2013. – V. 288. – P. 2848–2856.
11. Groenning M. Binding mode of Thioflavin T and other molecular probes in the context of amyloid fibrils—current status / M. Groenning // J. Chem. Biol. – 2010. – V. 3(1). – P. 1–18.
12. Bergelson L. Lipid-specific fluorescent probes in studies of biological membranes / L. Bergelson, J. Molotkovsky, Y. Manevich // Chem. Phys. Lipids. – 1985. – V. 37. – P. 165–195.
13. Lakowicz J. R. Principles of fluorescence spectroscopy / J. R. Lakowicz. - Springer: New York., 2006.
14. Bulychev A. A. Current methods of biophysical studies / A. A. Bulychev, V. N. Verchoturov, B. A. Gulaev. - Vyschaya shkola. Moscow., 1998.
15. Fung B.K. Surface density determination in membranes by fluorescence energy transfer / B. K. Fung, L. Stryer // Biochemistry. – 1978. – V. 17. – P. 5241–5248.
16. Effect of cholesterol on bilayer location of the class A peptide Ac-18A-NH2 as revealed by fluorescence resonance energy transfer / G. Gorbenko, T. Handa, H. Saito [et al.] // Eur. Biophys. J. 2003. – V. 32(8). – P. 703–709.
17. Dale R. The orientational freedom of molecular probes. The orientation factor in intramolecular energy transfer / R. Dale, J. Eisinger, W. Blumberg // Biophys. J. – 1979. – V. 26. – P. 161–193.
18. Differential study of phosphatidylcholine and sphingomyelin in human high-density lipoproteins with lipid-specific fluorescent probes / J. Molotkovsky, E. Manevich, E. Gerasimova [et al.] // Eur. J. Biochem. – 1982. – V. 122. – P. 573–579.
19. Structure of apolipoprotein A-I N terminus on nascent high density lipoproteins / J. O. Lagerstedt, G. Cavigiolio, M. S. Budamagunta [et al.] // J Biol Chem. – 2011. – V. 286. – P. 2966–2975.
20. Effects of the Iowa and Milano mutations on apolipoprotein A-I structure and dynamics determined by hydrogen exchange and mass spectrometry / P. S. Chetty, M. Ohshiro, H. Saito [et al.] // Biochemistry. – 2012. – V. 51(44). – P. 8993–9001.
21. Effects of a lipid environment on the fibrillogenic pathway of the N-terminal polypeptide of human apolipoprotein A-I, responsible for in vivo amyloid fibril formation / D. M. Monti, F. Guglielmi, M. Monti [et al.] // European Biophysics Journal. – 2010. – V. 39. – P. 1289–1299.
22. Babenko V. Thioflavin T forms a non-fluorescent complex with α-helical poly-L-glutamic acid / V. Babenko, W. Dzwolak // Chem. Commun. – 2011. – V. 47. – P. 10686–10688.
23. Solar M. Comparative analysis of nanomechanics of protein filaments under lateral loading / M. Solar, M. J. Buehler // Nanoscale. – 2012. – V. 21(4). – P. 1177–1183.
24. Robert T. Solid State NMR Studies of Amyloid Fibril Structure / T. Robert // Annu. Rev. Phys. Chem. – 2011. – V. 62. – P. 279–299.